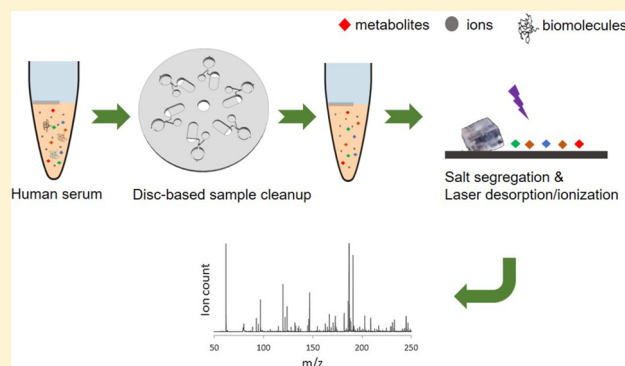


# Sample Preparation in Centrifugal Microfluidic Discs for Human Serum Metabolite Analysis by Surface Assisted Laser Desorption/Ionization Mass Spectrometry

Yufeng Zhao,<sup>†</sup> Yuting Hou,<sup>†</sup> Jing Ji,<sup>†</sup> Faheem Khan,<sup>‡</sup> Thomas Thundat,<sup>‡</sup> and D. Jed Harrison<sup>\*,†</sup><sup>†</sup>Department of Chemistry, University of Alberta, Edmonton, AB T6G 2G2, Canada<sup>‡</sup>Department of Chemical and Materials Engineering, University of Alberta, Edmonton, AB T6G 2R3, Canada

**ABSTRACT:** We introduce a centrifugal microfluidic disc that accepts a small volume in ( $\sim 5 \mu\text{L}$ ), performs sample cleanup on human serum samples, and delivers a small volume out, for subsequent metabolite analysis by surface assisted laser desorption/ionization (SALDI) mass spectrometry (MS) or hydrophilic interaction liquid chromatography (HILIC)-MS. The centrifugal microfluidic disc improves the MS results by removing proteins and lipids from serum. In the case of SALDI-MS, sample background electrolytes are segregated from analytes during the spotting process by the action of the SALDI-chip during drying, for further cleanup, while HILIC separates the salts in HILIC-MS. The resulting mass spectra of disc-prepared samples show a clean background and high signal-to-noise ratio for metabolite peaks. Several representative ionic metabolites from human serum samples were successfully quantified. The performances of the sample preparation disc for SALDI-MS and HILIC-MS were assessed and were comparable. Reproducibility, sample bias, and detection limits for SALDI-MS compared well to ultrafiltration sample preparation.



Metabolomic studies can facilitate biomarker discovery,<sup>1–4</sup> diagnosis of disease,<sup>5–9</sup> and toxic effect assessment of drugs, toxins, and food additives.<sup>10–14</sup> Considerable interest is focused on small-molecule metabolites ( $<1500 \text{ Da}$ ) such as amino acids,<sup>9,15,16</sup> lipids,<sup>17–19</sup> and fatty acids.<sup>15,20</sup> Once useful health markers are known, batch-processed, spot analyses are an attractive approach to routine assays. Analyzing blood-derived samples, such as serum, is of primary interest for metabolite assays,<sup>21</sup> but a high concentration of proteins, as well as other biomolecules, usually generates interferences in the following detection step, so sample preparation is required.

Here we introduce a centrifugal microfluidic device to prepare  $\sim 5 \mu\text{L}$  serum samples for small-molecule analysis by surface assisted laser desorption/ionization mass spectrometry (SALDI-MS). We have previously introduced a perfluoro-coated, vapor-deposited, nanoporous Si film for sample desalting and SALDI-MS.<sup>22</sup> Our centrifugal microfluidic disc, fabricated by a simple print, cut, and laminate method,<sup>23</sup> enables sample preparation, removing proteins and lipids from serum. The sample is recovered from the disc following cleanup and then transferred to a SALDI-chip, which provides an additional cleanup by segregating the electrolyte background from the sample salts.<sup>22</sup>

Conventional sample preparation methods for human serum include organic solvent precipitation and ultrafiltration.<sup>24–27</sup> Organic solvent precipitation methods take time and require that multiple steps be performed. Ultrafiltration<sup>22,28</sup> is often

conducted using commercial ultrafiltration centrifuge tubes, requiring a high-speed centrifuge and other standard laboratory steps, and is more challenging to use for low-volume samples ( $<25 \mu\text{L}$ ). Lower volume preparation and measurement of blood-derived samples allow for multiple tests from a single sample collection and would enable metabolite detection with capillary blood samples from finger-stick tests.

Microfluidic techniques for convenient small-volume biological sample preparation are often suggested but rarely realized. One of the challenges is that sample placed within a chip occupies too low a volume to be recovered for off-chip analysis, but integrating all of the detection components makes for an expensive single-use, disposable device. Microfluidic chips have been utilized for online separation in untargeted metabolomic profiling,<sup>29</sup> where samples were first prepared by various off-chip extraction/separation steps. Digital microfluidics has been utilized for sample preparation coupled with mass spectrometry in proteomic<sup>30–34</sup> and metabolite<sup>35,36</sup> studies. Digital microfluidics requires a sophisticated electronic control system for fluid manipulation and relatively high cost for device fabrication, and the range of sample processing steps that can be translated to that format has limitations. In contrast, centrifugal microfluidics features a simple control system and

Received: December 14, 2018

Accepted: May 15, 2019

Published: May 15, 2019

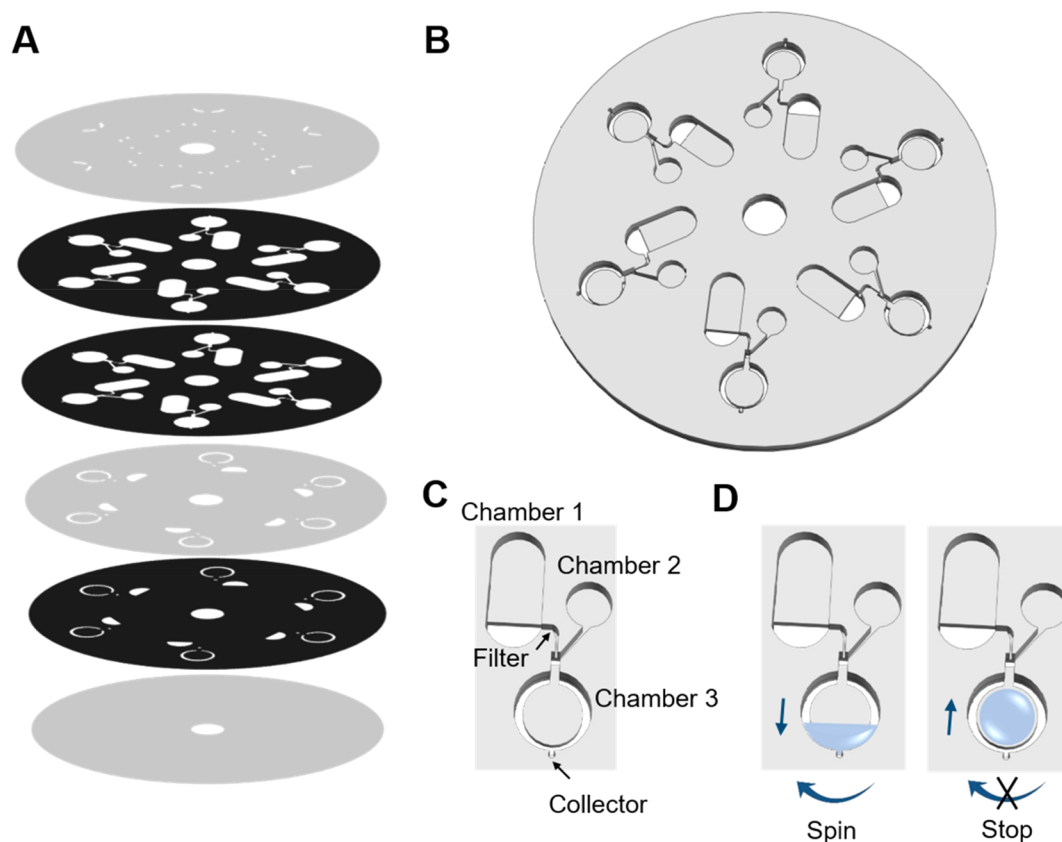


**Figure 1.** (A) Schematic representation of the centrifugal microfluidic device without assembly (six layers of polyester films). Transparencies with toners are shown in black, and transparencies without toners are shown in light gray. Features in the top layer include vents and sample inlets/outlets. (B) Assembled device without showing the top layer. (C) Design of a single sample processor. (D) Liquid movement in Chamber 3 under a spin–stop cycle.

inexpensive device fabrication, can duplicate many laboratory steps, and may facilitate high-throughput sample processing.<sup>37,38</sup> Proteomic applications of centrifugal microfluidics have been demonstrated for mass spectrometry,<sup>39</sup> although the sample cleanup challenges are different than for metabolites.<sup>40</sup> Sample preparation with centrifugal devices for the analysis of individual metabolites, such as glucose, alcohol, lactate, or uric acids, has been shown, with electrochemical<sup>41</sup> or optical detection.<sup>42,43</sup> However, sample preparation for mass spectrometry using centrifugal microfluidic devices for analysis of a broad range of small, ionic metabolites has not been reported.<sup>40</sup>

Here we have targeted free amino acids, which are critical in neurotransmission. Inoshita et al. found substantial elevated blood glutamate levels in major depressive disorder patients.<sup>44</sup> Concentration changes in free amino acids in probable Alzheimer's disease<sup>45</sup> were determined by Fonteh et al. in various biofluid samples. Citrate, whose level has been associated with cancer,<sup>46</sup> and taurine, which plays a crucial role in regulation of vasoactivity,<sup>47</sup> were also selected. We have compared the performance of the centrifugal sample preparation disc for sample cleanup for SALDI-MS with cleanup for LC/MS. The resulting mass spectrum of the prepared sample shows a relatively clean background and high signal-to-noise ratio (SNR) for metabolite peaks in SALDI-MS, and provides good sample cleanup for LC/MS. Reproducibility and recovery of several identified metabolites obtained from disc-based serum preparation with SALDI-MS detection are evaluated. Quantitative analysis of metabolites is demonstrated.

## EXPERIMENTAL SECTION

**Design of the Centrifugal Disc.** The centrifugal microfluidic device for human serum sample cleanup consists of six layers of polyester film with 10 cm diameter and 100  $\mu\text{m}$  thickness for each layer (Figure 1A). Layers 2, 3, and 5 (numbered from top to bottom) are printed with toner as bonding agent between layers. Features are cut by laser cutter, and layers are aligned and laminated by hot laminator, as described below. The assembled disc (Figure 1B) is fixed using a rubber cap on a spinning motor (0923/S010-R1, McMaster Carr), which is controlled by a DC power supply (6217A, Hewlett-Packard). The spinning frequency is measured by an RPM meter (1905T22, McMaster Carr). Figure 1C represents the microfluidic design of one processing unit on the disc for sample preparation, which includes three chambers. Chambers 1 and 2 are for sample and reagent introduction, respectively. A filter is inserted in the channel between chambers 1 and 3, to separate supernatant and pellets under filtration. Chamber 3 is a two-level structure with a shallow center area for sample drying and mixing. Sample stays in the center due to capillary force when the device is not spinning. When sample is being dried under vacuum, liquid will not contact with the edge of the chamber and enter the gap between layers. When the device is spinning and the centrifugal force overcomes the capillary force, the liquid sample will be driven to the outermost region in the chamber 3. Using spin–stop cycles, the liquid is moving to accelerate sample mixing (Figure 1D). A small collector at the far end of chamber 3 (shown at the bottom in Figure 1C) is

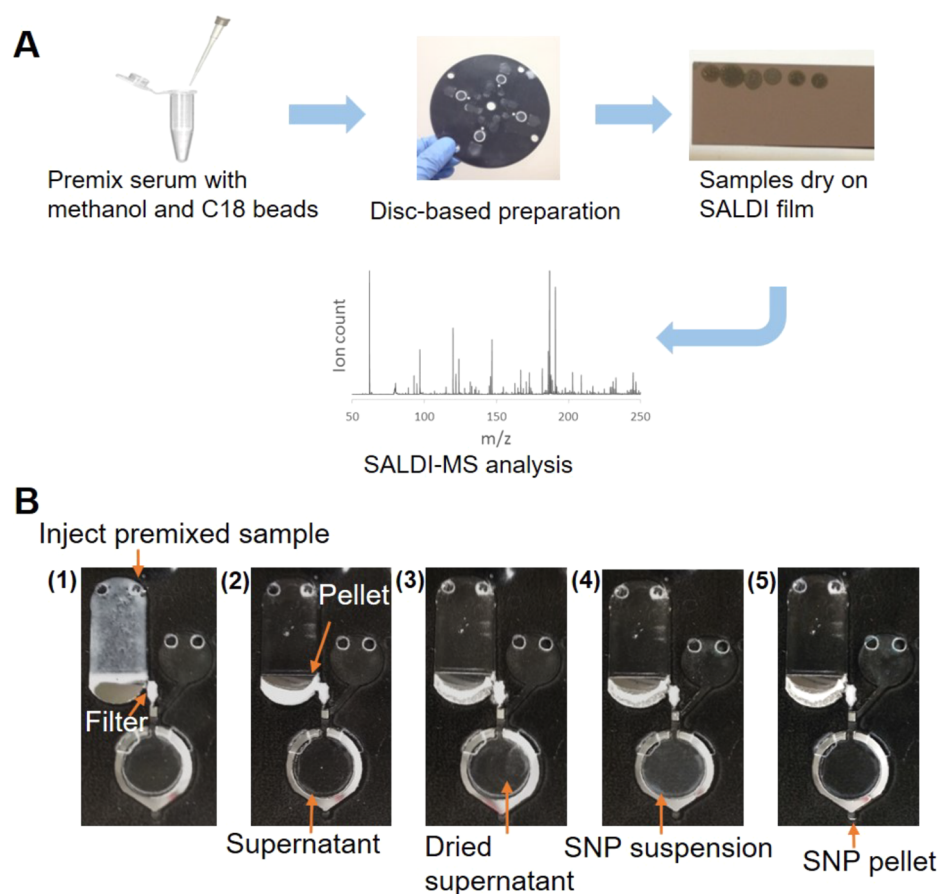


**Figure 2.** (A) Work flow of disc-based sample preparation and analysis of metabolites by SALDI-MS. (B) Images of disc-based preparation steps: (1) Inject serum samples premixed with methanol and C18 beads. (2) Pellet proteins and C18 beads by centrifugation and filtration. (3) Dry the supernatant by placing the disc in a vacuum chamber. (4) Add silica nanoparticle (SNP) suspension to dissolve the dried sample and adsorb remaining proteins in the sample. (5) Remove SNP by centrifugation.

used to collect silica nanoparticles by centrifugation, which are added to remove proteins in the sample.

**Fabrication of the Centrifugal Disc.** Centrifugal microfluidic discs were fabricated by a print, cut, and laminate method.<sup>23</sup> The  $8.5 \times 11$ " size transparency sheets (APO9209, APOLLO) were used as substrates for printing and laser cutting. For toner-printed transparency films, the whole area of each side was printed with three layers of black toner at a resolution of 600 dpi with the laser printer (HP LaserJet 2055dn). The DXF format file of the microfluidic design was created in AutoCAD software for laser cutting. Each layer of transparencies was fabricated by a CO<sub>2</sub> laser cutter (Epilog Legend) in the "Vector cutting" mode. The laser cutter was manually aligned, and cutting was performed with settings of 9% power, 80% speed, 1200 DPI, and 5000 Hz. The fabricated layers were removed from the rest of the transparencies, cleaned with ethanol and distilled water, and dried under N<sub>2</sub> before assembling. Transparency films were manually aligned and taped together with Scotch tape one layer at a time, from bottom to top. Before adding the top layer, a small piece ( $\sim 1 \times 1$  mm) of glass fiber filter (Whatman GF/B) was inserted. The assembled device was sandwiched between two layers of aluminum foil for hot lamination at 260 °F, with a Catena 35 laminator using 3 mm roller pressure and the lowest speed. The device was then removed from the foil and cooled for 1 min.

**SALDI-Chip Preparation.** The SALDI-chips were prepared as described previously.<sup>22</sup> Briefly, vertical silicon

nanoposts were deposited on a silicon wafer substrate by using glancing angle deposition (GLAD), followed by oxidation in an air environment and surface derivatization with (1*H*,1*H*,2*H*,2*H*-perfluorooctyl) dimethylchlorosilane (pFMe<sub>2</sub>SiCl, Gelest).

#### Sample Preparation Coupled with Offline SALDI-MS.

Figure 2A demonstrates the workflow of the sample preparation and detection. Pooled human serum sample (Innovative Research, MI) was first premixed with methanol (LC/MS grade, Fisher Chemical) and 10 μm C18 beads (S03207B, Silicycle) for 1 min, to precipitate proteins and extract lipids, respectively. C18 beads were suspended in methanol at a density of 0–10% (weight/volume) and a volume ratio of serum to C18 suspended methanol of 1:3. A 25 μL premixed sample was then prepared with the disc (Figure 2B). The precipitated proteins and C18 beads were separated from the liquid phase by the filter at 1500 rpm for 2 min. The supernatant containing the analytes was transferred into the two-level Chamber 3. The disc was then removed from the spinner and placed in a vacuum chamber to dry the supernatant for 20 min. After the sample was dried, 15 μL aqueous suspensions of 235 nm silica nanoparticles (microParticles GmbH, Germany), whose density was varied from 0 to 0.25% (weight/volume) during optimization, were added through chamber 2 to redissolve the dried sample and then mixed by spin–stop cycles for 3 min. The silica nanoparticles adsorbed the remaining proteins in the sample and were separated from

the solution by 2000 rpm centrifugation for 5 min, pelleted in the small collection region. The cleaned sample was pipetted out and acidified with 2 M HCl to reach a final concentration of 0.18 M HCl. A 1.8  $\mu$ L sample was then spotted onto a SALDI-chip in a Petri dish and dried at 4 °C overnight for salt crystallization.

The SALDI-chip with dried sample spots was attached to a customized MALDI plate with a double-sided conductive carbon tape (Electron Microscopy Sciences). The MALDI plate was inserted into an AB Sciex Voyager Elite MALDI-TOF mass spectrometer for analysis. A pulsed nitrogen laser (337 nm, 3 ns pulse) was employed for desorption and ionization. Mass spectra were acquired in negative-ion mode, and the signals were averaged for 100 laser shots, while the beam was rastered to fresh locations within the spot. For sample preparation assay development and analyte quantification, at least four replicate spots were measured to calculate the average value and standard deviation for each sample. The laser intensity for desorption and ionization was set to 2200 (a.u.) for C18 optimization and 2100 for other measurements. Other detailed instrument settings used previously optimized conditions.<sup>22</sup> Data Explorer 4.0 was used for MS data processing to calculate ion count intensity and SNR ratio.

Six metabolites, including taurine, aspartic acid, malic acid, glutamic acid, histidine, and citric acid, and two isotope-labeled metabolites, L-glutamic acid-<sup>15</sup>N and citric acid-1,5-<sup>13</sup>C<sub>2</sub>, were purchased from Sigma-Aldrich and prepared in deionized water (18.2 M $\Omega$ ) as standard solutions. Metabolites were quantified using the standard addition method. Briefly, serum samples were spiked with various volumes of standard solutions of analytes, followed by disc-based preparation and SALDI-MS detection. Isotope-labeled or endogenous metabolites were selected as internal standards.

**Clean Sample Recovery Test.** The disc-based preparation was divided into two steps, methanol/C18 treatment and silica nanoparticle treatment, for recovery evaluation of each step. Standard solutions were prepared containing a fixed concentration of isotope-labeled internal standards (200  $\mu$ M glutamic acid and 200  $\mu$ M citric acid) and various concentrations of non-isotope-labeled metabolites (0–500  $\mu$ M glutamic acid and 0–800  $\mu$ M citric acid). TBS buffer was run through the disc for preparation, 1:1 mixed with standards, acidified with HCl, and measured by SALDI for calibration curves. A clean sample with known concentrations of glutamic acid and citric acid in TBS buffer was prepared with the disc, using either the methanol/C18 or the silica nanoparticle extraction steps. The disc-prepared sample was mixed 1:1 with isotope-labeled internal standard solution, acidified with HCl to 0.18 M, measured by SALDI, and quantified according to calibration curves.

**Sample Preparation by Ultrafiltration.** Ultrafiltration of human serum samples was performed using centrifugal ultrafiltration tubes (Amicon Ultra-4, 3K Da cutoff) and the protocol described previously.<sup>22</sup> The ultrafiltered sample was acidified with HCl to reach a final concentration of 0.18 M HCl and then spotted on a SALDI-chip for drying and MS analysis. A standard addition method was employed for quantification with isotope-labeled internal standards.

**Hydrophilic Interaction Chromatography (HILIC) with MS.** A hydrophilic interaction chromatography column (Agilent InfinityLab Poroshell 120 HILIC-Z phase) was used to separate the amino acids, coupled with a positive-ion mode operated Single Quadrupole MS (Agilent Technologies 1100 HPLC with G1946A MSD) for detection. Isotope-labeled

glutamic acid served as internal standard and was spiked into serum samples before disc processing for glutamic acid quantification. All reagents were HPLC grade or higher. Water was purified using an EMD Millipore Milli-Q Integral System (Darmstadt, Germany). HPLC Mobile phase A was 25 mM ammonium formate in water at pH = 7.5, mobile phase B was 25 mM aqueous ammonium formate in 9:1 acetonitrile/water, the flow rate was 0.50 mL/min with an injection volume of 1  $\mu$ L, at a 25 °C column temperature. Quantitation of glutamic acid in serum was accomplished with a four-point calibration curve using ratios of peak areas at 6.56 min, for isotope-labeled Glu (147 Da) and native Glu (146 Da).

## RESULTS AND DISCUSSION

**Sample Preparation Assay Development for Serum Cleanup.** To identify a sample clean up process that can be realized on a centrifugal disc, we first considered existing sample preparation methods that remove proteins and lipids from serum samples. A widely used cleanup method for metabolomics in serum uses methanol precipitation of protein,<sup>48</sup> followed by liquid–liquid extraction with chloroform to extract hydrophobic molecules from the sample. The aqueous phase is then analyzed. Another common approach is to use ultrafiltration, which we employed for SALDI-MS previously, with acidification by HCl.

Methanol precipitation and supernatant collection is readily accomplished on a disc. However, chloroform can cause severe damage to the disc by dissolving the toners, so we replaced liquid–liquid extraction with solid phase extraction. As a first stage extraction, C18 beads suspended in methanol were mixed with serum with a volume ratio of 3:1 for protein precipitation and extraction. The supernatant, after mixing of serum, methanol, and C18 beads, was collected, dried under vacuum, and redissolved with the same volume of water for SALDI-MS detection. Particle densities of 1.7, 3.3, 6.6, and 10% were tested, the sample spots on SALDI-chips were observed by microscope, and the SNRs of six different metabolites were evaluated. Figure 3A shows that spots from sample preparation with 0 and 1.7% C18 beads (wt/vol % in methanol) are larger than sample spots prepared with higher density C18. For densities of 3.3% or higher, the contact angle of the spotted droplets is higher, the dried spots are cleaner, and background electrolyte crystallization is localized in larger crystals, allowing better mass spectrometry of the metabolites. Treating samples with 3.3% C18 beads improved the SNR of aspartic acid, glutamic acid, and histidine by a factor of 2 compared to methanol alone. A two-tailed *t* test shows that the SNRs for these three components, prepared with 3.3% C18, are improved from samples prepared with 1.7% C18 ( $p < 0.05$ ), but the SNR decreased again at higher particle density. Taurine and citric acid showed their best results at 1.7%, with a small decline at 3.3%. Malic acid showed the same response at 0 and 3.3% particle density. On the basis of this study, 3.3% C18 particle density was selected for the solid phase extraction step.

Additional steps may be required to further clean serum samples, as methanol precipitation cannot completely remove the proteins in serum.<sup>49,50</sup> Silica nanoparticles were selected for a second extraction stage, since they adsorb proteins in serum samples.<sup>51–54</sup> Mixing and separation of the nanoparticles was not difficult to realize on a centrifugal microfluidic platform. The effect of the size of the silica nanoparticles on protein adsorption has been studied previously, showing that smaller size nanoparticles with larger surface area adsorb more

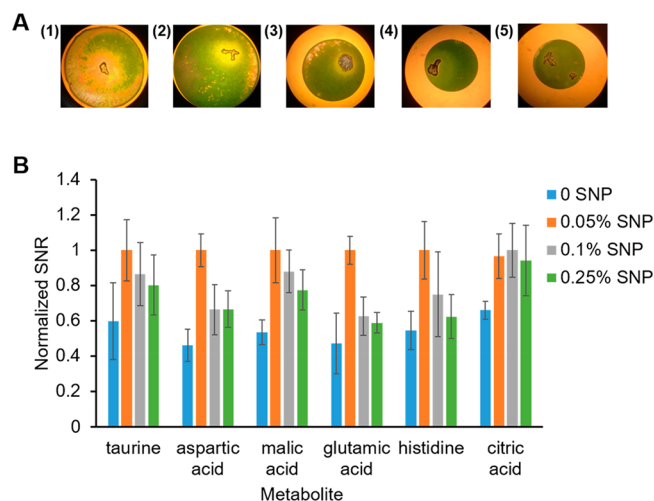


**Figure 3.** (A) Microscopic photos of serum samples prepared with methanol precipitation and solid phase extraction with different densities of C18 beads: (1) 0%; (2) 1.7%; (3) 3.3%; (4) 6.6%; (5) 10%. (B) Normalized signal-to-noise ratio of metabolites from serum samples prepared in a disc-based manner with different densities of silica nanoparticles (SNP) to remove proteins after disc-based methanol precipitation and C18 bead extraction. Error bars represent standard deviations of average.

proteins.<sup>51</sup> In our microfluidic device, particles with a diameter less than 200 nm took too long to remove by centrifugation, while particles with a diameter larger than 500 nm were difficult to mix in the spin-stop cycles, leading us to select 235 nm silica nanoparticles. Figure 3B illustrates the SNR of six metabolites in serum samples prepared with different densities (wt/vol % in methanol) of nanoparticles. Compared to preparation with methanol and C18 beads alone, 0.05% silica nanoparticles increase the SNR of all six metabolites by a factor of  $\sim 2$ , as confirmed by  $p < 0.05$  for the six metabolites. However, a higher density of silica nanoparticles leads to lower SNR. The net increase in SNR from the two optimized stages of C18 and silica extraction versus using methanol alone is  $\sim 4$ .

#### Mass Spectra of Disc-Based Sample Preparations.

Figure 4 illustrates the mass spectra of serum samples after disc-based preparation with the optimized methanol precipitation, C18, and silica particle cleanup method, versus laboratory-based ultrafiltration and acidification. The identified metabolite  $[M-H]$  peaks are labeled with their  $m/z$  values. The mass spectrum of the disc-based sample preparation (Figure 4 upper trace) gives a flat baseline, little noise, and tens of metabolite peaks, which is similar to the spectrum of the ultrafiltered sample (Figure 4, middle trace). The lower intensities of the metabolites for disc-based sample preparation compared to the ultrafiltered sample is mainly attributed to dilution in the disc-based preparation. The SNR of the six metabolites in disc-prepared samples is  $\sim 2$  times lower when compared to samples prepared by ultrafiltration. However, after methanol precipitation and C18 extraction, the sample is about  $4\times$  diluted and not concentrated again in the following steps. This dilution impacts the signal, but can be readily overcome by evaporation of the solvent and reconstitution in a smaller volume. The results establish that a useful mass spectrum can be obtained using the disc-based preparation, comparable to commonly employed laboratory-based methods.

To further evaluate the role of the C18 and silica treatment, a negative control was performed using disc-based methanol

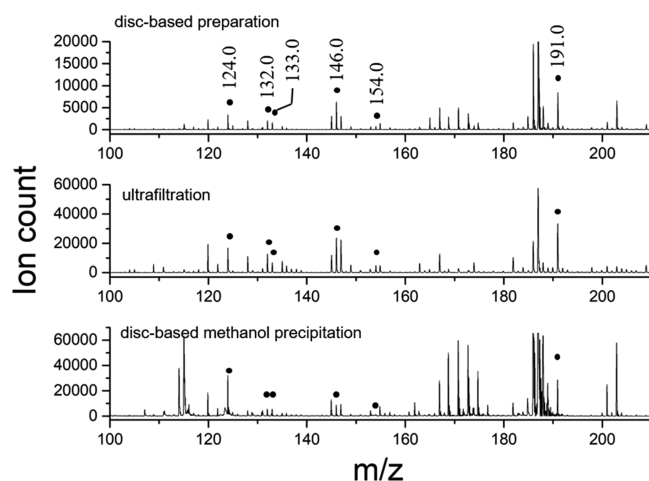


**Figure 4.** SALDI mass spectra (negative mode) of serum sample after preparation, with labeled peaks (taurine: 124.0; aspartic acid: 132.0; malic acid: 133.0; glutamic acid: 146.0; histidine 154.0; citric acid: 191.0), in the  $m/z$  range of 100–210. Upper plot, disc-based preparation with methanol, C18 and silica beads; central plot, ultrafiltration; lower plot, disc-based methanol precipitation with no bead based extraction.

precipitation alone, followed by SALDI of the aqueous reconstituted serum sample. The lower trace in Figure 4 shows a poor baseline, large background peaks, and low SNR for analytes, presumably because of incomplete removal of proteins and lipids. There are clusters of background peaks with strong intensities in several  $m/z$  regions, such as 170–175 and 185–190, which could be identified as false positive metabolite peaks or could result in false negatives for metabolites in this region because of the chemical noise. Figure 4 shows that the C18 and silica extraction steps greatly reduce the background peaks seen when using methanol alone, providing a spectrum that is much more similar to the ultrafiltration preparation. It is clear that the C18 and silica particle treatment contribute substantially to improved analytical performance.

**Quantification Using Isotope-Labeled Internal Standard.** Two metabolites, glutamic acid and citric acid, were selected for quantification by the standard addition method with isotope-labeled internal standards (<sup>15</sup>N glutamic acid and <sup>13</sup>C citric acid), as illustrated in Figure 5A,B. The SALDI-MS analytical results from disc-based serum sample preparations were 430  $\mu\text{M}$  for glutamic acid and 160  $\mu\text{M}$  for citric acid (Table 1). The same serum sample prepared by ultrafiltration and detected by SALDI-MS shows consistent results, 463 and 157  $\mu\text{M}$  for glutamic acid and citric acid, respectively (Table 1). The serum samples were also assayed by HILIC-MS, following disc-based sample preparation, and the result for glutamic acid was 405  $\mu\text{M}$ . The RSD is  $\sim 10\%$  in these analyses, meaning the concentrations observed by the three approaches are in reasonable agreement. (Citric acid interacts too strongly with the HILIC column to provide useful quantitative LC/MS results.)

**Analysis with Endogenous Internal Standard.** While isotope-labeled chemicals are ideal internal standards for mass-spectrometry-based metabolite analysis, the limited availability and relatively high cost of these chemicals provide challenges for analyzing large varieties of metabolites. Biological samples usually contain numerous endogenous small molecules with various physical and chemical properties, which hold great

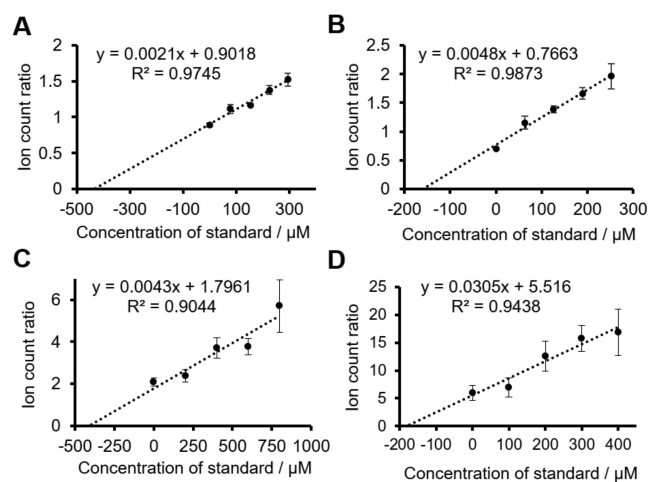


**Figure 5.** Calibration curves of glutamic acid (A,C) and citric acid (B,D) in serum samples prepared by a centrifugal microfluidic disc and detected on SALDI-chip with isotope-labeled (A,B) or endogenous (C,D) internal standards. Standard addition method was employed for quantitative analysis. Ion count ratio (analyte/internal standard) in each calibration curve is  $^{14}\text{N}$  glutamic acid/ $^{15}\text{N}$  glutamic acid (A),  $^{12}\text{C}$  citric acid/ $^{13}\text{C}$  citric acid (B), glutamic acid/glutamine (C), or citric acid/malic acid (D). Error bars represent the standard deviations of average.

**Table 1.** Comparison of the Quantitative Results for Metabolites in Human Serum Samples<sup>a</sup>

	concentration in original serum sample / $\mu\text{M}$		
	centrifugal disc-SALDI-MS	ultrafiltration-SALDI-MS	database <sup>e</sup>
taurine	70 <sup>b</sup>	72 <sup>d</sup>	45–130
aspartic acid	43 <sup>b</sup>	53 <sup>d</sup>	<25
malic acid	23 <sup>b</sup>	18 <sup>d</sup>	3–21
glutamic acid	430 <sup>c</sup>	463 <sup>c</sup>	<100
histidine	108 <sup>b</sup>	88 <sup>d</sup>	26–120
citric acid	160 <sup>c</sup>	157 <sup>c</sup>	30–400

<sup>a</sup>Prepared and quantified by centrifugal microfluidic disc-SALDI-MS with endogenous or isotope-labeled internal standards and by ultrafiltration-SALDI-MS. <sup>b</sup>Data quantified with endogenous internal standards, as shown in Figure 6. <sup>c</sup>Data quantified with isotope-labeled internal standards, as shown in Figure 5. <sup>d</sup>Data from reference 22. <sup>e</sup>Data from Human Metabolome Database (HMDB, [www.hmdb.ca](http://www.hmdb.ca)).

potential for serving as internal standards. And unlike in LC/MS, where using the same chemical with a different isotope is required to ensure the same elution time, in SALDI-MS, all masses are ionized simultaneously. We evaluated several endogenous internal standards for the metabolites we have studied, for both reproducibility and quantitative precision.

The reproducibility of the disc-based sample preparation method was assessed, with six parallel sample preparation experiments, performed in separate microfluidic units on two discs. The relative standard deviations in ion counts for six metabolites are summarized in Table 2. When referenced to endogenous internal standards, the ratio of intensities showed substantially improved RSD. Given their chemical differences, there is no single metabolite that is a satisfactory internal standard for all six metabolites, as shown in Table 2 when malic acid is used as the reference for all. The optimal choices observed are given in the table, where it can also be seen that

**Table 2.** Assessment of Reproducibility of Disc-Prepared Serum Samples

metabolite ( $m/z$ )	ion count	RSD	
		relative intensity <sup>a</sup> (reference metabolite)	relative intensity (malic acid)
taurine (124.0)	40%	18% (citric acid)	30%
aspartic acid (132.0)	11%	4% (glutamine <sup>b</sup> )	9%
malic acid (133.0)	12%	9% (aspartic acid)	-
glutamic acid (146.0)	5%	7% (glutamine)	18%
histidine (154.0)	17%	11% (aspartic acid)	17%
citric acid (191.0)	26%	15% (malic acid)	15%

<sup>a</sup>Relative intensity is the intensity ratio of metabolite and reference metabolite (internal standard). <sup>b</sup> $m/z$  of glutamine is 145.0.

taurine and citric acid show higher RSD relative to the other compounds.

Figure 5 shows a comparison of the standard addition calibration curves obtained with isotope-labeled internal standards, versus alternate endogenous internal standards (Figure 5A vs C, and 5B vs D). The extrapolated concentration values for glutamic acid and citric acid are in good agreement for both types of internal standard. The higher  $R^2$  values in the curve fits do indicate greater precision when using isotope-labeled internal standards, as expected with the isotope standards, but the performance of endogenous internal standards is nearly comparable.

Four additional metabolites in serum samples prepared with the disc were quantified by standard addition. Endogenous metabolites in serum were selected as internal standards for those analytes. The calibration curve for each metabolite was plotted as intensity ratio vs. concentration of standard (Figure 6). The results of quantification are summarized in Table 1, together with results obtained from a metabolite database as well as those from previous analysis of serum prepared by

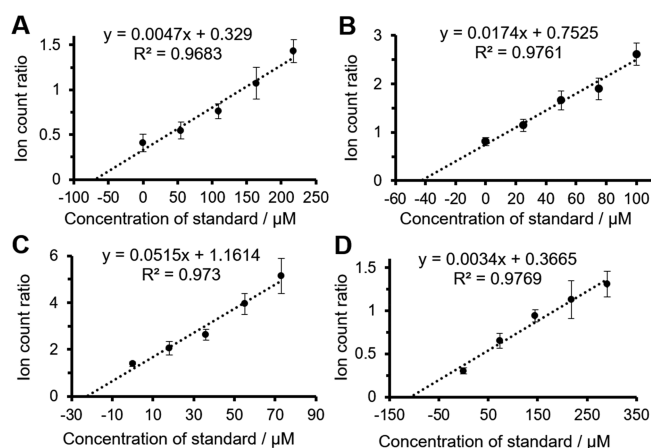


**Figure 6.** Calibration curves of taurine (A), aspartic acid (B), malic acid (C), and histidine (D) in serum samples prepared by centrifugal microfluidic disc and detected on SALDI-chip with endogenous internal standards. Standard addition method was employed for quantitative analysis. Ion count ratio (analyte/internal standard) in each calibration curve is taurine/citric acid (A), aspartic acid/glutamine (B), malic acid/aspartic acid (C), or histidine/aspartic acid (D). Error bars represent standard deviations of average.

**Table 3. Metabolite Recovery from Disc-Prepared Serum with Endogenous Internal Standards<sup>a</sup>**

metabolite	taurine	aspartic acid	malic acid	glutamic acid	histidine	citric acid
recovery/%	105 ± 16	87 ± 14	38 ± 3	101 ± 7	103 ± 26	28 ± 6

<sup>a</sup>Error represents the standard deviation of average.

ultrafiltration then quantified by SALDI-MS.<sup>22</sup> The results of all six metabolites were consistent with those from the other preparation and quantification methods. The limit of quantitation for the compounds evaluated here in serum were in the range of 0.5–5 μM, similar to our previous reports for GLAD films used for amino acid analysis.<sup>22</sup>

To evaluate the recovery of the six metabolites in the process of disc-based preparation, we analyzed and compared two groups of samples spiked with standards, either before or after preparation with a disc. Standards spiked in serum samples before preparation (Group 1) may suffer from losses during preparation, whereas standards spiked in the samples after preparation (Group 2) do not. Recovery was calculated as follows, assuming a linear relation between signal and concentration.  $S_1$  and  $S_2$  are the signals of a spiked metabolite from Group 1 and Group 2, respectively.  $S_0$  is the signal of a metabolite from a disc-prepared sample without spiking.

$$\text{recovery} = (S_1 - S_0)/(S_2 - S_0) \times 100\%$$

The recovery of each metabolite is summarized in Table 3. The recovery of malic acid and citric acid are significantly lower than those of the other four metabolites. Malic acid and citric acid have analogous chemical structures, containing one hydroxyl group and multiple carboxyl groups, which lead to different interactions with the beads in the preparation step.

To further understand the recovery observed, two isotope-labeled chemicals (<sup>15</sup>N glutamic acid and <sup>13</sup>C citric acid) were used to test recovery of the two non-isotope-labeled metabolites in “clean” buffer samples (analyte in pH 7.4 tris buffer). The two individual sample preparation steps, methanol precipitation with C18 treatment or silica nanoparticle treatments, were assessed separately. The results (Table 4)

**Table 4. Recovery of Metabolites for Each Individual Disc-Prepared Step<sup>a</sup>**

	methanol/C18	silica nanoparticles
glutamic acid	101 ± 2%	101 ± 5%
citric acid	27% ± 5%	99 ± 10%

<sup>a</sup>Determined in buffer, “clean samples” with isotope-labeled internal standards. Error represents the standard deviation of average value.

are in good agreement with the serum recovery experiments and show that the absence of protein did not change the observed recoveries. Glutamic acid shows no obvious loss from either of the sample preparation steps, while citric acid suffers from low recovery in the methanol/C18 step.

In using two solid phase extraction steps, there can be concern about a bias in the final concentration because of selective extraction. It is known that silica nanoparticles can adsorb some metabolites when protein is absent,<sup>55</sup> but in the presence of proteins, silica is not likely to adsorb metabolites, which is because of stronger interactions with proteins compared to metabolites.<sup>52</sup> The C18 phase may also result in some bias, and this is illustrated in the case of the citric acid. Given the use of standard addition and an internal standard as an approach, the impact of such bias can be reduced.

**Centrifugal Disc Preparation Coupled with LC/MS.** To explore the versatility of our disc preparation for different analytical methods, we combined the disc-based sample preparation of serum with HILIC-MS, using an isotope-labeled internal standard. As indicated above, the result for glutamic acid using disc-LC/MS was 405 μM, which is in agreement within experimental error of the results from disc-SALDI. The standard addition curve had an  $R^2$  of 0.943, similar to the plots for SALDI-MS, indicating a similar level of precision. (Interactions with the HILIC phase for citric and malic acids were very strong, showing strong tailing in the chromatograms, so an equivalent study with labeled citric acid was not performed.)

The HILIC-MS study was also used to establish that the  $m/z$  peaks assigned to various metabolites in the SALDI-MS data were correctly assigned and did not include other chemicals of a similar mass. HILIC-MS of metabolite standards established the elution times, while extracted ion chromatograms of disc-prepared serum samples showed only a single peak, at the same elution time.

## CONCLUSION

This work realizes the goal of producing sufficient processed sample volume from a microfluidic device for sample recovery and subsequent external laboratory measurement of the cleaned up sample. The strategy separates the low-cost, disposable, microfluidic device for sample preparation, from the detection elements, which can be costly or impossible to fabricate in a microfluidic system. The centrifugal disc device demonstrates sufficient removal of proteins, lipids, and other biomolecules for effective mass spectrometry of multiple small-ion metabolites in human serum samples. Disc-prepared serum samples were analyzed by both SALDI-MS and HILIC-MS, with similar performance characteristics. The results illustrate the potential usefulness of the centrifugal disc in sample preparation for more than one type of analytical measurement, with the target of specific metabolite assays or panels of metabolites for a specific disease.

## AUTHOR INFORMATION

### Corresponding Author

\*E-mail: jed.harrison@ualberta.ca; Phone: +1-780-492-2790.

### ORCID

Yufeng Zhao: 0000-0002-1788-7969

D. Jed Harrison: 0000-0002-1474-0910

### Notes

The authors declare no competing financial interest.

## ACKNOWLEDGMENTS

This work was supported by the Natural Sciences and Engineering Research Council of Canada (NSERC) and Alberta Innovates – Health Solutions. We thank Alberta Innovates Technology Futures for the scholarship to Yufeng Zhao and the University of Alberta for support of the NanoFab facility. We thank R Whittal for advice and support within the Chemistry Mass Spec Facility.

## REFERENCES

- (1) Schlotterbeck, G.; Ross, A.; Dieterle, F.; Senn, H. *Pharmacogenomics* **2006**, *7*, 1055–1075.
- (2) Wang, X.; Zhang, A.; Han, Y.; Wang, P.; Sun, H.; Song, G.; Dong, T.; Yuan, Y.; Yuan, X.; Zhang, M.; Xie, N.; Zhang, H.; Dong, H.; Dong, W. *Mol. Cell. Proteomics* **2012**, *11*, 370–380.
- (3) Kim, K.; Aronov, P.; Zakharkin, S. O.; Anderson, D.; Perroud, B.; Thompson, I. M.; Weiss, R. H. *Mol. Cell. Proteomics* **2009**, *8*, 558–570.
- (4) Griffiths, W. J.; Koal, T.; Wang, Y.; Kohl, M.; Enot, D. P.; Deigner, H. *Angew. Chem., Int. Ed.* **2010**, *49*, 5426–5445.
- (5) Emwas, A. M.; Salek, R. M.; Griffin, J. L.; Merzaban, J. *Metabolomics* **2013**, *9*, 1048–1072.
- (6) Mickiewicz, B.; Vogel, H. J.; Wong, H. R.; Winston, B. W. *Am. J. Respir. Crit. Care Med.* **2013**, *187*, 967–976.
- (7) Tiziani, S.; Lopes, V.; Günther, U. L. *Neoplasia* **2009**, *11*, 269.
- (8) Wen, H.; Yoo, S. S.; Kang, J.; Kim, H. G.; Park, J.; Jeong, S.; Lee, J. I.; Kwon, H. N.; Kang, S.; Lee, D.; Park, S. J. *Hepatology* **2010**, *52*, 228–233.
- (9) Miyagi, Y.; Higashiyama, M.; Gochi, A.; Akaike, M.; Ishikawa, T.; Miura, T.; Saruki, N.; Bando, E.; Kimura, H.; Imamura, F.; Moriyama, M.; Ikeda, I.; Chiba, A.; Oshita, F.; Imaizumi, A.; Yamamoto, H.; Miyano, H.; Horimoto, K.; Tochikubo, O.; Mitsushima, T.; Yamakado, M.; Okamoto, N. *PLoS One* **2011**, *6*, No. e24143.
- (10) Dong, H.; Zhang, A.; Sun, H.; Wang, H.; Lu, X.; Wang, M.; Ni, B.; Wang, X. *Mol. BioSyst.* **2012**, *8*, 1206–1221.
- (11) Jones, O. A. H.; Spurgeon, D. J.; Svendsen, C.; Griffin, J. L. *Chemosphere* **2008**, *71*, 601–609.
- (12) Wang, X.; Wang, H.; Zhang, A.; Lu, X.; Sun, H.; Dong, H.; Wang, P. *J. Proteome Res.* **2012**, *11*, 1284–1301.
- (13) Roessner, U.; Patterson, J. H.; Forbes, M. G.; Fincher, G. B.; Langridge, P.; Bacic, A. *Plant Physiol.* **2006**, *142*, 1087–1101.
- (14) West, P. R.; Weir, A. M.; Smith, A. M.; Donley, E. L. R.; Cezar, G. G. *Toxicol. Appl. Pharmacol.* **2010**, *247*, 18–27.
- (15) Mihalik, S. J.; Michaliszyn, S. F.; de las Heras, J.; Bacha, F.; Lee, S.; Chace, D. H.; DeJesus, V. R.; Vockley, J.; Arslanian, S. A. *Diabetes Care* **2012**, *35*, 605–611.
- (16) Lindsay, K. L.; Hellmuth, C.; Uhl, O.; Buss, C.; Wadhwa, P. D.; Koletzko, B.; Entringer, S. *PLoS One* **2015**, *10*, No. e0145794.
- (17) Oliveira, A. R.; Silva, I.; LoTurco, E.; Martins, H.; Chauffaille, M. L. *Blood* **2014**, *124*, 5958.
- (18) Cai, X.; Li, R. *Sci. Rep.* **2016**, *6*, 36490.
- (19) Sampey, B. P.; Freerman, A. J.; Zhang, J.; Kuan, P.; Galanko, J. A.; O'Connell, T. M.; Ilkayeva, O. R.; Muehlbauer, M. J.; Stevens, R. D.; Newgard, C. B.; Brauer, H. A.; Troester, M. A.; Makowski, L. *PLoS One* **2012**, *7*, No. e38812.
- (20) Lam, C.; Law, C. J. *Proteome Res.* **2014**, *13*, 4040–4046.
- (21) Zhang, A.; Sun, H.; Wang, X. *Anal. Bioanal. Chem.* **2012**, *404*, 1239–1245.
- (22) Zhou, Y.; Peng, C.; Harris, K. D.; Mandal, R.; Harrison, D. J. *Anal. Chem.* **2017**, *89*, 3362–3369.
- (23) Thompson, B. L.; Ouyang, Y.; Duarte, G. R. M.; Carrilho, E.; Krauss, S. T.; Landers, J. P. *Nat. Protoc.* **2015**, *10*, 875–886.
- (24) Bruce, S. J.; Jonsson, P.; Antti, H.; Cloarec, O.; Trygg, J.; Marklund, S. L.; Moritz, T. *Anal. Biochem.* **2008**, *372*, 237–249.
- (25) Michopoulos, F.; Lai, L.; Gika, H.; Theodoridis, G.; Wilson, I. J. *Proteome Res.* **2009**, *8*, 2114–2121.
- (26) Zelena, E.; Dunn, W. B.; Broadhurst, D.; Francis-McIntyre, S.; Carroll, K. M.; Begley, P.; O'Hagan, S.; Knowles, J. D.; Halsall, A.; HUSERMET, C.; et al. *Anal. Chem.* **2009**, *81*, 1357–1364.
- (27) Pereira, H.; Martin, J.; Joly, C.; Sébédio, J.; Pujos-Guillot, E. *Metabolomics* **2010**, *6*, 207–218.
- (28) Psychogios, N.; Hau, D. D.; Peng, J.; Guo, A. C.; Mandal, R.; Bouatra, S.; Sinelnikov, I.; Krishnamurthy, R.; Eisner, R.; Gautam, B.; Young, N.; Xia, J.; Knox, C.; Dong, E.; Huang, P.; Hollander, Z.; Pedersen, T. L.; Smith, S. R.; Bamforth, F.; Greiner, R.; McManus, B.; Newman, J. W.; Goodfriend, T.; Wishart, D. S. *PLoS One* **2011**, *6*, No. e16957.
- (29) Tharakan, R.; Tao, D.; Ubaida-Mohien, C.; Dinglasan, R. R.; Graham, D. R. *J. Proteome Res.* **2015**, *14*, 1621–1626.
- (30) Luk, V. N.; Wheeler, A. R. *Anal. Chem.* **2009**, *81*, 4524–4530.
- (31) Moon, H.; Wheeler, A. R.; Garrell, R. L.; Loo, J. A.; Kim, C. C. *Lab Chip* **2006**, *6*, 1213–1219.
- (32) Wheeler, A. R.; Moon, H.; Bird, C. A.; Ogorzalek Loo, R. R.; Kim, C. C. J.; Loo, J. A.; Garrell, R. L. *Anal. Chem.* **2005**, *77*, 534–540.
- (33) Jebrail, M. J.; Wheeler, A. R. *Anal. Chem.* **2009**, *81*, 330–335.
- (34) Luk, V. N.; Fiddes, L. K.; Luk, V. M.; Kumacheva, E.; Wheeler, A. R. *Proteomics* **2012**, *12*, 1310–1318.
- (35) Jebrail, M. J.; Yang, H.; Mudrik, J. M.; Lafrenière, N. M.; McRoberts, C.; Al-Dirbashi, O.; Fisher, L.; Chakraborty, P.; Wheeler, A. R. *Lab Chip* **2011**, *11*, 3218–3224.
- (36) Abdelgawad, M.; Watson, M. W. L.; Wheeler, A. R. *Lab Chip* **2009**, *9*, 1046–1051.
- (37) Gorkin, R.; Park, J.; Siegrist, J.; Amasia, M.; Lee, B. S.; Park, J.; Kim, J.; Kim, H.; Madou, M.; Cho, Y. *Lab Chip* **2010**, *10*, 1758–1773.
- (38) Strohmeier, O.; Keller, M.; Schwemmer, F.; Zehnle, S.; Mark, D.; von Stetten, F.; Zengerle, R.; Paust, N. *Chem. Soc. Rev.* **2015**, *44*, 6187–6229.
- (39) Gustafsson, M.; Hirschberg, D.; Palmberg, C.; Jörnvall, H.; Bergman, T. *Anal. Chem.* **2004**, *76*, 345–350.
- (40) Kraly, J. R.; Holcomb, R. E.; Guan, Q.; Henry, C. S. *Anal. Chim. Acta* **2009**, *653*, 23–35.
- (41) Li, T.; Fan, Y.; Cheng, Y.; Yang, J. *Lab Chip* **2013**, *13*, 2634–2640.
- (42) Grumann, M.; Steigert, J.; Riegger, L.; Moser, I.; Enderle, B.; Riebeseel, K.; Urban, G.; Zengerle, R.; Ducrée, J. *Biomed. Microdevices* **2006**, *8*, 209–214.
- (43) Steigert, J.; Grumann, M.; Brenner, T.; Riegger, L.; Harter, J.; Zengerle, R.; Ducrée, J. *Lab Chip* **2006**, *6*, 1040–1044.
- (44) Inoshita, M.; Umehara, H.; Watanabe, S.; Nakataki, M.; Kinoshita, M.; Tomioka, Y.; Tajima, A.; Numata, S.; Ohmori, T. *Neuropsychiatr. Dis. Treat.* **2018**, *14*, 945–953.
- (45) Fonteh, A. N.; Harrington, R. J.; Tsai, A.; Liao, P.; Harrington, M. G. *Amino Acids* **2007**, *32*, 213–224.
- (46) Mycielska, M.; Milenkovic, V.; Wetzl, C.; Rümmele, P.; Geissler, E. *Curr. Mol. Med.* **2015**, *15*, 884–891.
- (47) Abebe, W.; Mozaffari, M. S. *American journal of cardiovascular disease* **2011**, *1*, 293.
- (48) Nagana Gowda, G. A.; Raftery, D. *Anal. Chem.* **2014**, *86*, 5433–5440.
- (49) Bruce, S. J.; Tavazzi, I.; Parisod, V.; Rezzi, S.; Kochhar, S.; Guy, P. A. *Anal. Chem.* **2009**, *81*, 3285–3296.
- (50) Crowe, K. M. *Clin. Biochem.* **2014**, *47*, 116–118.
- (51) Hata, K.; Higashisaka, K.; Nagano, K.; Mukai, Y.; Kamada, H.; Tsunoda, S.; Yoshioka, Y.; Tsutsumi, Y. *Nanoscale Res. Lett.* **2014**, *9*, 668.
- (52) Zhang, B.; Xie, M.; Bruschweiler-Li, L.; Bruschweiler, R. *Anal. Chem.* **2016**, *88*, 1003–1007.
- (53) Lynch, I.; Dawson, K. A. *Nano Today* **2008**, *3*, 40–47.
- (54) Treuel, L.; Nienhaus, G. U. *Biophys. Rev.* **2012**, *4*, 137–147.
- (55) Zhang, B.; Xie, M.; Bruschweiler-Li, L.; Bingol, K.; Bruschweiler, R. *Anal. Chem.* **2015**, *87*, 7211–7217.

## NOTE ADDED AFTER ASAP PUBLICATION

This paper was originally published ASAP on May 31, 2019. The third author's name was changed from M. Faheem Khan to Faheem Khan, and the paper was reposted on June 3, 2019.